

MOLECULAR SIMULATIONS OF DYNAMIC PROCESSES OF SOLID EXPLOSIVES

Betsy M. Rice*

U. S. Army Research Laboratory, AMSRD-ARL-WM-BD
Aberdeen Proving Ground, MD 21005-5069

Dan C. Sorescu

U. S. Department of Energy, National Energy Technology Laboratory, Pittsburgh, PA 15236

Vinayak Kabadi

North Carolina A&T State University, Greensboro, North Carolina 27411

Paras M. Agrawal

Oklahoma State University, Stillwater, OK 74074

Donald L. Thompson

University of Missouri, Columbia, MO

ABSTRACT

A variety of molecular dynamics simulations of energetic materials is presented, demonstrating the ability to predict structural and thermodynamic properties of these materials. The studies are also used to explore, at an atomic level, dynamic processes that might influence conversion of the material to products. These studies are presented to illustrate how information generated through molecular dynamics simulations can be used in the design, development and testing of energetic materials.

1. INTRODUCTION

The chemically interesting features of energetic materials have been advantageously employed in a wide variety of industrial and military applications, but often these utilizations have not been fully optimized. This was mainly due to the inability to identify and understand the individual fundamental physical and chemical steps that control the conversion of the material to its final products. The conversion of the material is usually not the result of a single-step reaction, or even a set of a few simple consecutive chemical reactions. Rather, it is an extremely complex process in which numerous chemical and physical events occur in a concerted and synergistic fashion, and whose reaction mechanisms are strongly dependent on a wide variety of factors. Direct measurements of mechanistic details that would provide a fundamental description of the conversion process are lacking due to substantial experimental obstacles. These difficulties have required the development of innovative theoretical methods and models designed to probe details of the various phenomena associated with the conversion of energetic materials to products. Toward this end, we have expended considerable effort in developing and critically assessing a realistic generalized model for use in

molecular simulations of dynamic processes of condensed phase explosives.

Our development of the model follows an evolutionary approach. We first start with a simple description of interatomic interactions between molecules, and apply the model in condensed phase molecular simulations in which each molecule is treated as a rigid entity. Several studies were performed to explore the ability of the model to reproduce structural and thermodynamic information, and to determine limits of this model and the rigid-molecule assumption when applied to various classes of CHNO explosives. Results indicate that within the low-pressure, low temperature regime, such an approximation is adequate for predicting structural and thermodynamic information.

The next stage in our model development is to incorporate flexibility (not reaction) of the molecules into the model. Several simulations of increasing complexity have been performed to assess this extended model, and are summarized herein. These include investigations of nitromethane over the entire temperature ranges of both solid and liquid phases, and over large pressure ranges (0-14 GPa) in both phases, melting, and vibrational energy relaxation (VER) in liquid nitromethane after excitation of the C-H stretching vibrations.

Our ultimate goal is to simulate conversion of the material to products at conditions of extreme temperatures and pressures; our next step in the model development will incorporate chemical reactivity. However, it is imperative that the chemical and physical events immediately preceding the conversion be accurately depicted. In this paper, we report numerous studies in which we have assessed such depictions, and describe lessons learned in the development of this generalized model of CHNO explosives.

Report Documentation Page

Form Approved
OMB No. 0704-0188

Public reporting burden for the collection of information is estimated to average 1 hour per response, including the time for reviewing instructions, searching existing data sources, gathering and maintaining the data needed, and completing and reviewing the collection of information. Send comments regarding this burden estimate or any other aspect of this collection of information, including suggestions for reducing this burden, to Washington Headquarters Services, Directorate for Information Operations and Reports, 1215 Jefferson Davis Highway, Suite 1204, Arlington VA 22202-4302. Respondents should be aware that notwithstanding any other provision of law, no person shall be subject to a penalty for failing to comply with a collection of information if it does not display a currently valid OMB control number.

1. REPORT DATE 00 DEC 2004	2. REPORT TYPE N/A	3. DATES COVERED -			
4. TITLE AND SUBTITLE Molecular Simulations Of Dynamic Processes Of Solid Explosives		5a. CONTRACT NUMBER			
		5b. GRANT NUMBER			
		5c. PROGRAM ELEMENT NUMBER			
6. AUTHOR(S)		5d. PROJECT NUMBER			
		5e. TASK NUMBER			
		5f. WORK UNIT NUMBER			
7. PERFORMING ORGANIZATION NAME(S) AND ADDRESS(ES) U. S. Army Research Laboratory, AMSRD-ARL-WM-BD Aberdeen Proving Ground, MD 21005-5069; U. S. Department of Energy, National Energy Technology Laboratory, Pittsburgh, PA 15236		8. PERFORMING ORGANIZATION REPORT NUMBER			
		10. SPONSOR/MONITOR'S ACRONYM(S)			
9. SPONSORING/MONITORING AGENCY NAME(S) AND ADDRESS(ES)		11. SPONSOR/MONITOR'S REPORT NUMBER(S)			
		12. DISTRIBUTION/AVAILABILITY STATEMENT Approved for public release, distribution unlimited			
13. SUPPLEMENTARY NOTES See also ADM001736, Proceedings for the Army Science Conference (24th) Held on 29 November - 2 December 2005 in Orlando, Florida. , The original document contains color images.					
14. ABSTRACT					
15. SUBJECT TERMS					
16. SECURITY CLASSIFICATION OF:			17. LIMITATION OF ABSTRACT UU	18. NUMBER OF PAGES 8	19a. NAME OF RESPONSIBLE PERSON
a. REPORT unclassified	b. ABSTRACT unclassified	c. THIS PAGE unclassified			

2. DETAILS OF THE CALCULATIONS

2.1. Molecular Simulation Methods

The classical molecular simulation methods of molecular dynamics (MD) and molecular packing (MP) have been used to study the static and dynamic properties of energetic materials. These methods are limited by the classical approximation and an accurate description of the potential energy surface (PES) for the system. An MD simulation involves integrating equations of motion to generate temporal profiles of atomic positions and velocities, thus providing a dynamic description of the system. Also, thermodynamic information can be obtained by averaging properties evaluated at each integration step over the duration of the simulation. Molecular packing is an atomistic simulation method that is used to investigate structural features and properties very near local minima on the PES, and involves minimization of crystalline lattice energies by varying crystallographic parameters. MP cannot produce dynamic information; rather it provides information about equilibrium structures.

2.2. Potential Energy Surface (PES)

Our initial model, hereafter denoted as the SRT model after the original authors (Sorescu et al., 1997), assumed that the potential energy used in this study for a system of N molecules can be described as the sum of intermolecular interaction terms:

$$V_{Total} = \frac{1}{2} \sum_{i=1}^N \sum_{j=1}^N V_{ij}^{intermolecular} \quad (1)$$

The intermolecular potential i consists of the superposition of a pairwise sum of Buckingham (6-exp) (repulsion and dispersion) and Coulombic (C) potentials of the form:

$$V_{\alpha\beta}(r) = A_{\alpha\beta} \exp(-B_{\alpha\beta}r) - C_{\alpha\beta} / r^6 \quad (2)$$

and

$$V_{\alpha\beta}^C(r) = \frac{q_{\alpha}q_{\beta}}{4\pi\epsilon_0 r}, \quad (3)$$

where r is the interatomic distance between atoms α and β , q_{α} and q_{β} are the electrostatic charges on the atoms, and ϵ_0 is the dielectric permittivity constant of free space.

The set of partial charges used in these calculations were determined through fitting these to the quantum-mechanically derived electrostatic interaction potential for an isolated molecule whose atoms are arranged in the experimental crystallographic arrangement. The remaining exponential-six parameters were adjusted to reproduce the experimental structure of the RDX crystal at ambient conditions (Sorescu et al., 1997).

The simple model, which does not have a description of intramolecular motions such as bond stretches, angle bends or torsional motions, can be used only in simulations in which the molecule is rigid. This model is suitable for calculations of simple thermodynamic and structural properties for low temperature and pressure regimes, where deformation of the molecule is not important. Assuming the rigid-molecule approximation significantly reduces computational expenses in simulations due to the elimination of costly terms in the interaction potential that describe molecular flexibility. However, regimes of extreme temperatures and pressures are of great importance in the study of energetic materials, and inclusion of molecular flexibility is required in order to study processes within these regimes. Thus, a subsequent important step was the extension of the SRT intermolecular potential to include the full intramolecular (non-reactive) interactions. This has been done for the case of the nitroalkane explosive, nitromethane. The modifications were simple additions of intramolecular terms to describe stretching, bending and torsional motions. These terms were parameterized using quantum mechanical information of the isolated molecule.

3. RESULTS

3.1 Rigid Molecule Simulations

In addition to reproducing the crystal structure of RDX at ambient conditions using both MP and MD techniques (Sorescu et al., 1997), we found that this interaction potential could also describe the geometric parameters and lattice energies of different polymorphic phases of two other nitramine crystals: the polycyclic nitramine HNIW (CL-20) (Sorescu et al. 1998a) and the monocyclic nitramine HMX (Sorescu et al. 1998b). Further investigations exploring the limits of transferability of this interaction potential to other energetic molecular crystals were undertaken by performing molecular packing calculations for 30 nitramine crystals (Sorescu et al. 1998c) and 51 non-nitramine CHNO crystals (Sorescu et al. 1999a). MP calculations using this interaction potential reproduced the crystal structures of all of these to within 5% of experiment. An extremely important result of the MP studies was the sensitivity of the results upon the selection of the partial charges used in the study. As discussed in Section 2.2, these charges have been determined from fits to *ab initio* electrostatic potentials calculated for the individual molecules whose atoms are arranged in the experimental configurations. We have considered four different electrostatic models, with charges determined at a variety of levels of quantum mechanical theory: Hartree-Fock (HF), gradient-corrected non-local Density Functional Theory using the B3LYP density functional (B3LYP), second order second-order Möller-Plesset

perturbation theory (MP2) and charges calculated at the HF level uniformly scaled by a factor of 0.9. There is only a small influence (generally less than 1%) on the crystallographic parameters by the set of electrostatic charges used. However, the lattice energies of the crystals are significantly influenced by the electrostatic model. In particular, the best agreement with the experimental lattice energies has been obtained for the MP2 charges. The lattice energies calculated using the B3LYP charges overestimate the MP2 energies by about 2.6% while the HF charges overestimate the MP2 energies by 13.6%. The procedure of uniformly scaling the HF charges by the 0.9 factor decreases the above differences to about 6.2%. Lattice energies calculated for the HMX, CL-20, TNT and PETN systems all support polymorphic stability rankings determined experimentally (Sorescu et al., 1998a, 1998b, 1998c, 1999a).

The next step in model development was to explore the validity of the rigid-molecule assumption in simulations of energetic materials under hydrostatic compression. Therefore, we analyzed the dynamics of the energetic crystals RDX, HMX, HNIW and PETN under hydrostatic compression conditions using isothermal-isobaric (NPT) MD simulations and this simple intermolecular potential (Sorescu et al., 1999b). In that study, predicted lattice parameters for the RDX, HMX and HNIW crystals were found in good agreement with experimental values over the entire range of pressures investigated experimentally. For the PETN crystal, the calculated crystallographic parameters were in acceptable agreement with experimental data only for pressures of a few GPa. For higher pressures, the disagreements of predictions with experiment demonstrated the inadequacy of the rigid-body approximation when used in simulations of floppy molecules such as PETN.

This effect is illustrated in Figure 1, in which the calculated volumes of the RDX and PETN crystals are plotted as functions of pressure, and compared with experiment. While the MP predictions, which do not include thermal effects, are in some disagreement with experiment, the NPT-MD simulations of RDX are in very good agreement with experiment over the range of pressures explored. However, the failure of the model to predict crystal densities of PETN under high compression is quite apparent. Therefore, the SRT results suggest that at moderate temperatures and pressures, simulations using the rigid-molecule approximation will provide reasonably accurate results at a significantly reduced computational cost compared to those that use more complex flexible interaction potentials.

3.2 Structural studies of flexible nitromethane in the solid and liquid phase

Sorescu, Rice, and Thompson extended the original SRT model by adding an intramolecular part which consists of a superposition of bond stretching, bond bending and torsional angle terms (Sorescu et al., 2000). In particular, Morse potentials have been used to represent bond stretches while harmonic and cosine type of potentials have been used to simulate the bending and torsional motions. These terms were parameterized based on the geometric and vibrational frequencies and the corresponding eigenvectors data obtained from ab initio molecular orbital calculations for the isolated molecule. Molecular packing calculations using the proposed potential produce an accurate prediction of the crystallographic parameters with deviations less than 1.2% for the lattice edges. Moreover, NPT-MD simulations performed over the temperature range 4.2-228 K and pressure range 0.3-7.0 GPa indicate that the crystallographic parameters are well reproduced for the entire range of temperatures and pressures simulated.

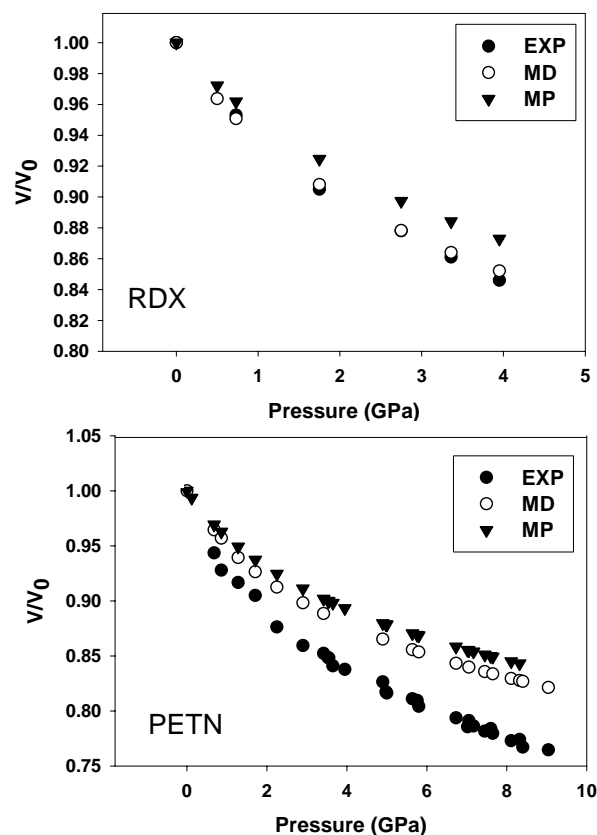


Figure 1. Comparison of the dependence of volume compression V/V_0 on the external pressure obtained in MP and NPT-MD simulations for the α -RDX crystal (upper frame) and PETN (lower frame) with the experimental results.

Excellent agreement was found for the calculated bulk modulus of nitromethane (6.78 GPa) with the experimental data (7.0 GPa). The corresponding predicted values as a function of either temperature or

pressure reproduce very well the experimental data obtained by neutron diffraction techniques (Trevino and Rymes, 1980) or by X-ray diffraction (Cromer et al., 1985). Further, the data agree very well with the experimental findings in which the methyl group was found to be rotated by about 45° relative to the low temperature configuration. Figure 2 shows the time averaged distributions of the three H-C-N-O dihedral angles in nitromethane, averaged over all molecules in the simulation cell, as functions of temperature and pressure. The distributions show that at 1 atm for all temperatures studied, the orientation of the methyl group oscillates about its equilibrium position determined at 4.2 K, 1atm. However, the peaks of the distributions shift with increases in pressure at $T=293$ K. At low pressures, the distributions indicate that the orientation of the methyl groups are the same as that of the low-temperature, low-pressure crystal. There is a continuous shift of the peak positions with pressure such that between 0.3 GPa and 5.4 GPa this shift amounts to about 41° while between 0.3 GPa and 7.0 GP the corresponding variation is about 50° . Also, the corresponding activation energy for methyl rotation was found to be in the range of the reported experimental activation energies.

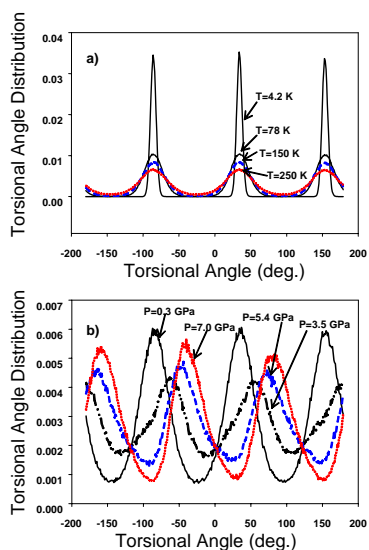


Figure 2. Distribution of the $H_i-C_1-N_2-O_3$ ($i=5,6,7$) dihedral angles for all nitromethane molecules in the simulation box as function of temperature (1 atm) (a) and pressure ($T=293$ K) (b).

In a subsequent study, the transferability of the general intra- and inter-molecular potential developed for crystalline nitromethane to the liquid phase of nitromethane was explored by computing various physical properties of the liquid as functions of temperature and pressure (Sorescu et al., 2001). A large set of static and dynamic properties of liquid nitromethane have been considered in these tests including the heat of

vaporization, the variation of density with temperature (over the range 255-374 K) and pressure (over the range 0-14.2 GPa), the thermal expansion coefficient, the self-diffusion coefficients, the viscosity coefficient, the dielectric constant, the bulk modulus, and the variation of vibrational frequencies with pressure. The analyses performed using NPT-MD simulations show that the great majority of these structural, energetic and spectroscopic are well reproduced. The only exception is the dielectric permittivity, which was underestimated. This limitation was attributed to the lack of polarization effects in the intermolecular interactions.

3.3 Melting of nitromethane

Melting of nitromethane was also explored using the SRT model using two types of MD simulations. The first type of simulation is one in which the crystal is gradually heated until a parameter that monitors the degree of translational order in the crystal abruptly decreases. This change indicates that the system has transitioned from the crystalline to the liquid state, and the temperature at which this occurs is the “transition” temperature (see Figure 3).

MD simulations using this method for several atomic crystals have shown that the transition temperature for a perfect crystal is substantially higher than the true thermodynamic melting temperature, but that the introduction of a critical number of voids lowers the transition temperature near the true thermodynamic melting point (Solca et al., 1997, 1998; Agrawal et al., 2003b). Therefore, the key assumption in this method is that the true thermodynamic melting temperature for any model corresponds to the transition temperature for a crystal containing a critical concentration of voids. The calculated value of the melting temperature for the nitromethane model using this method is in good agreement with experiment; however, because this method of predicting the thermodynamic melting point is empirical, a second melting simulation was performed in which a coexistence of the liquid and solid phases were simulated to confirm the result.

For this method, a simulation cell was constructed in which a block of liquid nitromethane was appended to a rectangular block of crystalline nitromethane, and the system equilibrated (using NPT-MD) to the desired temperature and pressure. Once equilibrated, NVE-MD simulations were performed and the temperature and behavior of the system monitored. If the temperature of the system is too high, the solid portion of the crystal will melt. If the temperature of the system is below the melting point, the liquid portion of the cell will solidify. The melting point is the temperature for which the liquid and solid maintain a coexistence. The results for the two methods were in near agreement, with the slight difference being attributed to hysteresis associated with

the direct heating process imposed in the void-nucleated melting simulation.

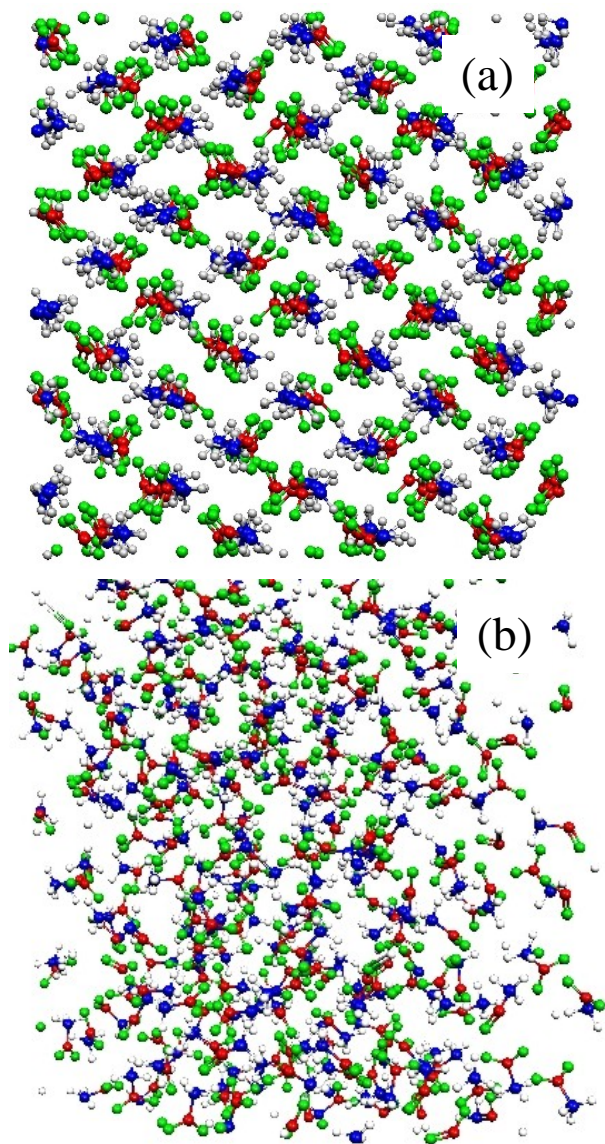


Figure 3: Snapshot of nitromethane crystal resulting from molecular dynamics simulations before (top) and after (bottom) reaching the melting point.

The values of the calculated melting temperature, T_m , are found to be in good agreement with the experimental data at various values of pressure ranging from 1 atm to 30 kbar (Figure 4). The computed values of the melting temperature satisfy the Simon-Glatzel equation: $P(\text{kbar}) = aT_m^b + c$, where $a = 1.597 \times 10^{-5}$, $b = 2.322$, $c = -6.74$, and T_m is in Kelvin. A comparison of computed T_m with and without the presence of molecular vibrations reveals that T_m is insensitive to the intramolecular interaction term of the potential energy function, but depends strongly on the intermolecular interactions, particularly the Coulombic term (i.e., the partial charges on atoms).

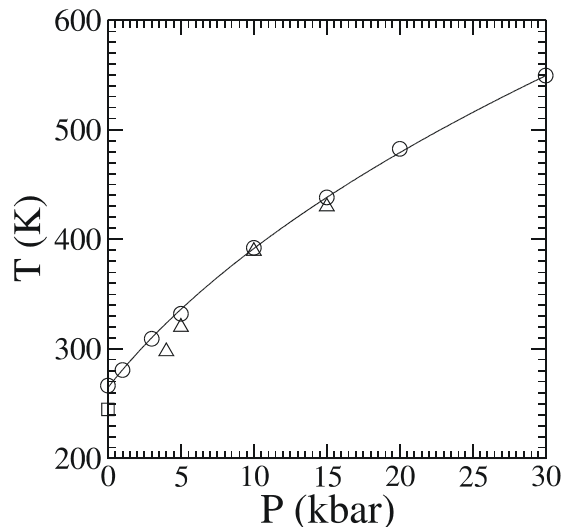


Figure 4: Pressure (in kbar) versus the melting temperature T (in K). The circles denote computed melting points, the line is a fit of the computed points to the Simon-Glatzel equation, the rectangles are experimental melting points reported by Jones and Giauque (Jones and Giauque, 1947) and the triangles denote the experimental values of Piermarini et al. (Piermarini et al., 1989).

3.4 Energy transfer in liquid nitromethane

Non-equilibrium molecular dynamics simulations were used to study vibrational energy relaxation (VER) in liquid nitromethane after excitation of the C-H stretching vibrations. This study was designed to explore the role of multiphonon up pumping in shock initiation of energetic materials, a theory based on mechanisms of energy flow in a shocked system. The multiphonon up pumping process begins with the heating of the phonons of a material upon the passage of a shock wave. The excess energy of the phonons flows into the cold molecular modes of the material through low-frequency modes that are strongly coupled to the phonon bath, and whose frequencies are near that of the maximum frequency of the phonon continuum (Chen et al., 1994).

As energy continues to flow from the overheated phonon bath into the doorway vibrations, higher-energy vibrational modes are subsequently excited through intramolecular vibrational energy transfer. This “up pumping” of vibrational states continues until sufficient energy is localized in the reaction coordinates of the molecules to allow reactions. Dlott and co-workers have performed extensive experimental investigations of energy transfer in condensed phase molecular systems to assess various aspects of this theory (Chen et al., 1994, 1995; Hong et al., 1995; Deak et al. 1999; Dlott, 2001).

Dlott and co-workers have performed a series of spectroscopic studies of vibrational energy relaxation (VER) in liquid nitromethane (NM) that have demonstrated that the VER process in this system is fairly complex (Chen et al., 1994, 1995; Hong et al., 1995; Deak et al. 1999; Dlott, 2001). The most recent study (Deak et al., 1999) used anti-Stokes Raman spectroscopy to measure instantaneous vibrational populations of NM after infrared excitation in the C-H stretching region (near 2970 cm^{-1}) for the neat liquid. Deak et al. (Deak et al., 1999) report that this pulse excites the C-H stretching vibrations and the first overtones of the antisymmetric CH_3 bending and NO_2 stretching vibrations. Additionally, this IR-Raman method was applied to solutions of NM-CCl_4 to extract details of energy flow that could not be obtained from experiments on the neat liquid. CCl_4 is transparent at 2970 cm^{-1} ; thus, it was used as a “molecular thermometer” to monitor the excitation of the bath upon vibrational cooling (VC) of NM. Monitoring the populations of CCl_4 vibrations after pump pulse excitation of the NM provided insight into the mechanism of VC for NM. The data show that the relaxation takes place in three steps. First, energy deposited in the C-H stretch (and in the first overtones of the antisymmetric NO_2 stretching and CH bending vibrations) is redistributed to all other vibrations within a few picoseconds. The NM-CCl_4 results do not reflect excitation of the CCl_4 during this time, indicating that the initial VER is intramolecular. Subsequently, the higher energy vibrations of NM (1560 and $\sim 1400\text{ cm}^{-1}$) relax on the time scale of $\sim 15\text{ ps}$, mainly by populating the lower energy vibrations (all transitions below $\sim 1400\text{ cm}^{-1}$). Approximately one-third of the energy from the decay of these two transitions is dissipated to the bath. Finally, the lower energy vibrations excited in the first two stages relax by heating the bath. VC of NM occurs on the 50 to 100 ps time scale, with the response of the CCl_4 vibrational transitions after excitation of the NM rising on the same time scale. This indicates that the excitation of the bath molecules occurs mainly through indirect intermolecular vibrational energy transfer (IVET) processes.

In an attempt to simulate the Deak et al. experiments (Deak et al., 1999) using classical MD, we utilized projection methods to follow the energy flow from excited molecular vibrational modes. In order to generate a fully-equilibrated liquid at the conditions of the experiment before excitation, an NPT MD simulation at 294 K 1 atm was performed. Next, a microcanonical MD simulation of liquid NM was performed, in which a percentage of the molecules in the equilibrated liquid were selected for mode-specific excitation. We did not identify information in the experimental papers that would allow us to quantify the populations of the various vibrational states that are excited from the mid-IR pulse. Since we did not have quantitative information on

vibrational populations, we arbitrarily chose to excite 120 molecules (25% of the total number in the simulation cell) with the excitation energy equipartitioned among the three CH stretching vibrations. Each excited molecule was given a total of 2.075 kcal/mol in the form of kinetic energy equally partitioned among the three CH stretching modes, thus introducing an excess energy corresponding to a temperature rise of 12.4 K , a value that is close to the experimental temperature jump resulting from the pump pulses in neat NM ($\sim 10\text{ K}$).

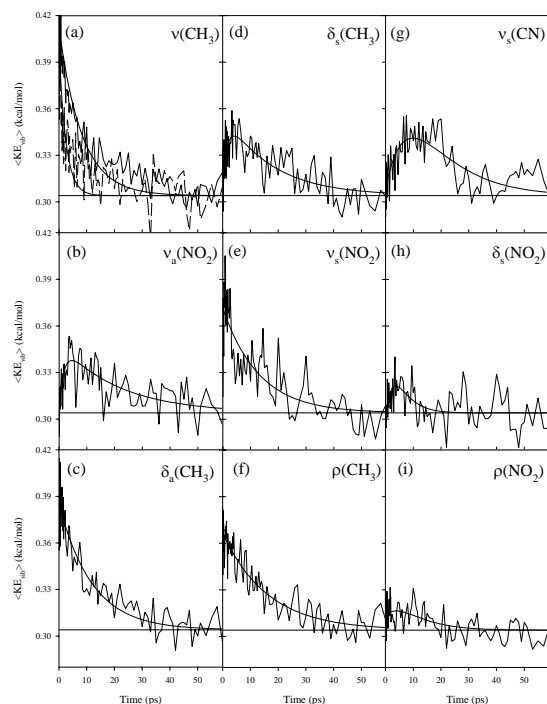


Figure 4. Average kinetic energies for normal modes (a) $\nu(\text{CH}_3)$; (b) $\nu_a(\text{NO}_2)$; (c) $\delta_a(\text{CH}_3)$; (d) $\delta_s(\text{CH}_3)$; (e) $\nu_s(\text{NO}_2)$ (f) $\rho(\text{CH}_3)$; (g) $\nu_s(\text{CN})$; (h) $\delta_s(\text{NO}_2)$; and (i) $\rho(\text{NO}_2)$ of the excited nitromethane molecules.

If the energy initially given to each molecule was immediately redistributed equally among its vibrational degrees of freedom, then the kinetic energy of vibration of each mode would increase from 0.292 to 0.341 kcal/mol . The information shown in Figure 4 indicates that such an immediate and uniform redistribution does not occur. Immediate increases in kinetic energy in all vibrational modes upon relaxation of the C-H stretches is evident. However, the differences in the curves show that energy transfer into the modes occurs at different rates, indicating that VC occurs in stages. The decay of the C-H stretching vibrational modes is exponential; however, the CH_3 symmetric stretch [Fig. 4(a)] has a VER lifetime of 2.5 ps , whereas the CH_3 asymmetric stretching mode has a VER lifetime that is ~ 3 times longer. The CH_3 asymmetric bends [Fig. 4(c)], NO_2 symmetric stretch [Fig. 4(e)] and CH_3 rocks [Fig. 4(f)] achieve their maximum level of excitation of ~ 0.37 - 0.38 kcal/mol almost immediately.

Energy flow from these vibrational modes occurs exponentially, with decay constants ranging from 11.9 to 16.2 ps. Four vibrational modes in the mid- to low-frequency range reach their maximum level of excitation at ~4 ps. The higher-frequency CH₃ symmetric bend [Fig. 4(d)] and NO₂ asymmetric stretch [Fig. 4(b)] attain a maximum kinetic energy of 0.34 kcal/mol at 4 ps, and the lower-frequency NO₂ symmetric bend [Fig. 4(h)] and rocking modes [Fig. 4(i)] attain a maximum energy of ~0.32 kcal/mol at 3.8 ps. Energy transfer from these modes can also be described as an exponential decay, but the lifetime of the low-frequency modes is much shorter than those of the higher frequency modes. The CN stretch mode [Fig. 4(g)] reaches its maximum excitation at 10 ps; energy flow from this point in time can be described as an exponential decay with lifetime ~20 ps. Although the kinetic energy for this mode appears to have reached the expected equilibrated value at 40 ps, the energy flow back into the mode, suggesting that it has not fully relaxed.

The profiles of the vibrational modes of the unexcited NM molecules as functions of time indicate that some VER from the excited NM to the bath occurs at the beginning of the VC process, though the degree of excitation is not great and the energy appears to be uniformly distributed among the vibrational modes. The behavior of the curves supports an indirect mechanism of IVET, characterized by Deak et al. (Deak et al., 1999) as a two-step process in which VC of the vibrationally hot NM excites the phonons in the liquid, which subsequently excite vibrations of the solvent molecules by multiphonon up-pumping.

Overall, the results are in qualitative agreement with experimental measurements of VER in liquid nitromethane after mid-IR excitation in the C-H stretching region. The simulation results indicate that the excited C-H stretching vibrations deposit energy predominantly into the remaining vibrations in the molecules. These vibrations relax at different rates, resulting in a multi-stage vibrational cooling process for nitromethane, in agreement with experimental results. The excitation of vibrations of the surrounding unexcited molecules occurs through indirect rather than direct intermolecular vibrational energy transfer processes, also in agreement with experiment. The main discrepancy between the experimental results and our results on the effect on the bath is the time scale on which the heating of the bath occurs. The experiments showed that while some energy buildup in the bath occurs on the 15 ps time scale, the majority of heating occurs on the 50-100 ps time scale corresponding to the final step of VC. The simulations show heating of the bath begins immediately, with full equilibration by 60 ps.

3.5 Shock Hugoniot of Nitromethane

The shock Hugoniot of a material provides a characterization of the behavior of a shock wave in that material, and is often used to assess performance of an explosive. The Hugoniot states are those that satisfy the Hugoniot relation (Zeldovich and Raizer, 1966)

$$H = E - E_0 - \frac{1}{2}(P + P_0)(V_0 - V) = 0 \quad (1)$$

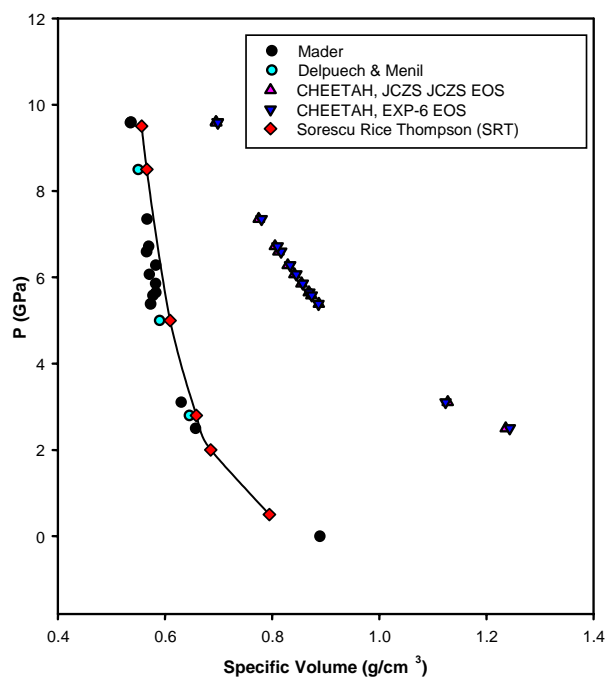


Figure 5. Shock Hugoniot of nitromethane. Calculated values from NPT-MD simulations using the SRT model are compared with experimental data (Mader, 2002; Delpuech and Menil, 1983) and results of thermochemical calculations using CHEETAH (Fried et al., 1998). The shock pressure is plotted versus the specific volume.

where E and V are the specific internal energy and volume, respectively, and P is the pressure. The term *specific* refers to the quantities normalized to unit mass and the subscript “o” denotes the quantity in the quiescent, unshocked material.

The equation of state of nitromethane described by the SRT potential was calculated using NPT-MD simulations; these results were used to calculate its shock Hugoniot. Results are shown in Fig. 5, along with experimental data and results calculated using the conventional thermochemical code CHEETAH and two different Equations of State. As evident in the figure, the Hugoniot curves predicted by CHEETAH using standard EOS are significantly different than that predicted by the SRT potential and experiment, and cannot adequately describe this system.

CONCLUSIONS

Overall, the above results indicate that a wide variety of properties can be predicted by using molecular simulations and the SRT model. We expect that further extensions of the model to describe other systems and to allow breaking and formation of bonds will result in full atomistic description of the initiation and conversion of real energetic materials to final products.

REFERENCES

- Agrawal, P.M.; Rice, B. M. and Thompson, D. L., 2003a: Molecular dynamics study of the melting of nitromethane, *J. Chem. Phys.* **119**, 9617.
- Agrawal, P.M.; Rice, B. M. and Thompson, D. L., 2003b: Molecular dynamics study of the effects of voids and pressure in defect-nucleated melting simulations, *J. Chem. Phys.* **118**, 9680.
- Chen, S.; Tolbert W. A. and Dlott, D. D., 1994: Direct measurement of ultrafast multiphonon up-pumping in high explosives, *J. Phys. Chem.* **98**, 7759.
- Chen, S.; Hong, X.; Hill, J. R. and Dlott, D. D., 1995: Ultrafast energy-transfer in high explosives – vibrational cooling, *J. Phys. Chem.* **99**, 4525.
- Cromer, D. T.; Ryan, R. R. and D. Schiferl, 1985: The structure of nitromethane at pressures of 0.3 to 6.0 GPa, *J. Phys. Chem.* **89**, 2315.
- Deak, J. C.; Iwaki, L. K. and Dlott, D. D., 1999: Vibrational energy redistribution in polyatomic liquids: Ultrafast IR-Raman spectroscopy of nitromethane, *J. Phys. Chem. A* **103**, 971.
- Delpuech, A. and Menil, A., 1983: Raman Scattering Temperature Measurement Behind a Shock Wave, *Shock Waves in Condensed Matter*, Asay, J.R., Graham, R. A. and Straub, G. K., ed, Elsevier Publishers, B.V.
- Dlott, D. D., 2001: Vibrational energy redistribution in polyatomic liquids: 3D infrared-Raman spectroscopy, *Chem. Phys.* **266**, 149.
- Fried, L. E.; Howard, W. M. and Clark Souers, P., 1998: *Cheetah 2.0 User's Manual*, UCRL-MA-117541 Rev. 5.
- Hong, X.; Chen, S. and Dlott, D. D., 1995: Ultrafast mode-specific intermolecular vibrational energy transfer to liquid nitromethane, *J. Phys. Chem.* **99**, 9102.
- Jones, W. M. and Giaque, W. F., 1947: The entropy of nitromethane – heat capacity of solid and liquid, vapor pressure, heats of fusion and vaporization, *J. Am. Chem. Soc.* **69**, 983.
- Kabadi, V.N. and Rice, B.M., 2004: Molecular dynamics simulations of normal mode vibrational energy transfer in liquid nitromethane, *J. Phys. Chem.* **108**, 532.
- Mader, C., LASL Shock Hugoniot Data, in *Numerical Modeling of Explosives and Propellants*, 2002.
- Piermarini, G. J.; Block, S. and Miller, P. J., 1989: Effects of pressure on the thermal decomposition kinetics and chemical reactivity of nitromethane, *J. Phys. Chem.* **93**, 457.
- Solca, J.; Dyson, A. J.; Steinebrunner, G. and Kirchner, B., 1997: Melting curve for argon calculated from pure theory, *Chem. Phys.* **224**, 253.
- Solca, J.; Dyson, A. J.; Steinebrunner, G.; Kirchner, B. and Huber, H., 1998: Melting curves for neon calculated from pure theory, *J. Chem. Phys.* **108**, 4107.
- Sorescu, D. C.; Rice, B. M. and Thompson, D. L., 1997: Intermolecular potential for the hexahydro-1,3,5-trinitro-1,3,5-s-triazine crystal (RDX): A crystal packing, Monte Carlo, and molecular dynamics study, *J. Phys. Chem., B* **101**, 798.
- Sorescu, D. C.; Rice, B. M. and Thompson, D. L., 1998a: Molecular packing and NPT molecular dynamics investigation of the transferability of the RDX intermolecular potential to 2,3,6,8,10,12-hexanitrohexaazaisowurtzitane, *J. Phys. Chem. B* **102** 948.
- Sorescu, D. C.; Rice, B. M. and Thompson, D. L., 1998b: Isothermal-isobaric molecular dynamics simulations of 1,3,5,7-tetranitro-1,3,5,7-tetraazacyclooctane (HMX) crystals, *J. Phys. Chem. B* **102** 6692.
- Sorescu, D. C.; Rice, B. M. and Thompson, D. L., 1998c: A transferable intermolecular potential for nitramine crystals, *J. Phys. Chem. A* **102**, 8386.
- Sorescu, D. C.; Rice, B. M. and Thompson, D.L., 1999a: Molecular packing and molecular dynamics study of the transferability of a generalized nitramine intermolecular potential to non-nitramine crystals, *J. Phys. Chem. A* **103**, 989.
- Sorescu, D. C.; Rice, B. M. and Thompson, D. L., 1999b: Theoretical studies of the hydrostatic compression of RDX, HMX, HNIW, and PETN crystals, *J. Phys. Chem. B* **103**, 6783.
- Sorescu, D. C.; Rice, B. M. and Thompson, D. L., 2000: Theoretical studies of solid nitromethane, *J. Phys. Chem. B* **104**, 8406.
- Sorescu, D. C.; Rice, B. M. and Thompson, D. L., 2001: Molecular dynamics simulations of liquid nitromethane, *J. Phys. Chem. B* **105**, 9336.
- Trevino, S. F. and Rymes, W. H., 1980: A study of methyl reorientation in solid nitromethane by neutron scattering, *J. Chem. Phys.* **73**, 3001.
- Zeldovich, Y. B. and Raizer, Y. P., 1966: *Physics of Shock Waves and High-Temperature Hydrodynamic Phenomena*, Academic Press, New York.